React & Wind Nb_3Sn Common Coil Dipole

R. Gupta, M. Anerella, J. Cozzolino, J. Escallier, G. Ganetis, A. Ghosh, M. Harrison, J. Muratore, W. Sampson and P. Wanderer

Abstract— **This paper presents a summary of the design, construction and test results of a common coil dipole DCC017 made using "React & Wind" Nb_3Sn technology. It reached the computed short sample field of 10.2 T at 10.8 kA after a number of quenches. In order to build high field magnets with brittle pre-reacted superconductors one must develop magnet designs, tooling and construction techniques that keep conductor degradation due to bending and handling to a tolerable level. The successful construction and test of this magnet demonstrates that it is possible to design and build magnets in the 10 (plus) T range using "React & Wind" technology. The magnet is based on a 2-layer common coil design with a clear horizontal space of 31 mm. A unique feature of the design is a tall 338 mm clear vertical open space that can facilitate possible flat racetrack coil testing in a high background field without dis-assembling the magnet.**

Index Terms— **Accelerator magnets, High field magnets, React & wind technology, Superconducting magnets.**

I. Introduction

ALL presently known high field superconductors are brittle in nature. However, the fact that these materials become brittle only after the composite is reacted (heat treated) offers two distinct approaches: "React & Wind" and "Wind & React". The "React & Wind" approach allows a variety of materials (including insulation) to be used since the coil and associated structure are not subjected to high reaction temperature. Moreover, the "React & Wind" technology is expected to be more dependable for length scale-up. This is because in "React & Wind" approach, the coil package is not subjected to the high- temperature reaction cycle and hence there is no build-up of differential thermal expansion of different materials in the coil composite which will be proportional to length in "Wind & React" approach.

The major challenge with "React & Wind" approach has been to develop magnet designs and manufacturing techniques that do not put excessive strain on the brittle reacted conductor during the construction of the coil. It is for this reason that almost all high field Nb_3Sn short R&D accelerator magnets have been built with "Wind & React" technology. The 10.2 T magnet described in this paper is the highest field "React & Wind" Nb_3Sn accelerator R&D magnet ever built. So far, no Nb_3Sn full-length high field accelerator magnet has been built for any machine using either the "React & Wind" or the "Wind & React" technology. Successful construction and test of this magnet opens the possibility of using the "React & Wind" approach for longer magnets.

This paper presents a summary of the design, construction and test results of a "React & Wind" Nb_3Sn common coil dipole. The common coil dipole design [1] is a "conductor friendly" 2-in-1 design with large bend radii and is particularly suited for "React & Wind" technology. A deliberately conservative approach was chosen during the construction since the major purpose of building this R&D magnet was to determine the viability of the "React & Wind" approach in high field Nb_3Sn magnets. The amount of instrumentation (voltage taps, etc.) was kept to a minimum to eliminate the chance of potential damage. Moreover, no attempt was made to optimize field quality. Detailed descriptions of the magnet design, development of "React & Wind" and associated technology, and the magnet engineering have been described elsewhere [2]-[4]. A number of common coil R&D dipoles using "React & Wind" technology have also been built and tested at Fermilab [5], [6]. Nb_3Sn magnets using cosine theta designs "React & Wind" have also been built earlier [7], [8].

II. Design

The magnet is based on two pairs of flat racetrack coils made with pre-reacted Nb_3Sn cable. Stainless steel collars in combination with the stainless steel shell and the iron yoke contain the Lorentz forces. The coils are subjected to only minimal pre-stress in the horizontal, vertical and axial directions when cold. An internal electrical splice was incorporated to facilitate a change in relative current grading between the inner and outer layers for potential future tests. A brief review of the magnetic and mechanical design of the magnet is given below.

A. Magnetic Design

The magnetic design consisted of two layers of coil in a 2-in-1 common coil configuration [1] with a minimum bend radius of 70 mm. Major parameters of the design are given in Table I. One quadrant of the magnet cross-section (one half of one aperture) is shown in Fig. 1 and a 3-d model is shown in Fig. 2. To take full advantage of the modular nature of the common coil design, all coil modules were deliberately made as identical single layer mechanical cassettes with one splice

Manuscript received August 28, 2006; last revised November 30, 2006.

All authors are associated with Brookhaven National Laboratory, Upton, NY 11973 USA. E-mail address of the corresponding author is gupta@bnl.gov and phone number is (631)344-4805.

TABLE I
MAJOR PARAMETERS OF REACT & WIND COMMON COIL DIPOLE DCC017

Magnet design	2-in-1 common coil dipole
Conductor type	Nb_3Sn
Magnet technology	React and wind
Horizontal coil aperture (clear space)	31 mm
Vertical coil aperture (clear space)	338 mm
Separation between upper and lower aperture	220 mm
Number of layers	Two
Number of turns per quadrant of single aperture (pole-to-pole)	45 turns in each layer
Coil height (pole-to-pole)	85 mm
Wedge(s) (size and number)	8.5 mm, one in each layer (inner & outer)
End-spacer(s) (size and number)	8.5 mm, one in each layer (inner & outer)
Wire non-Cu J_{sc} (4.2 K, 12 T)	1900 A/mm^2
Strand diameter	0.8 mm
Number of strands in inner and outer cable	30
Cable width in inner and outer layer	13.13 mm
Cu/Non-Cu ratio in the wire of inner and outer cable	1.53
Computed quench current	10.8 kA
Computed quench field @4.2 K (including cable degradation)	10.2 T
Peak field at quench in inner, outer Layer	10.7 T, 6.1 T
Coil bobbin (core) material	Carbon steel
Coil length (overall)	620 mm
Coil straight section length	305 mm
Coil inside radius in ends	70 mm
Coil outside radius in ends	155 mm
Coil curing preload - sides	0 N
Coil curing preload – ends	0 N
Cable insulation thickness	180 µm thick Nomex®
Potting agent	CTD-101K
Thickness of the collar	26.6 mm
Stainless steel shell thickness	25.4 mm
Thickness of the end plates	127 mm
Yoke outer radius	267 mm
Yoke length	653 mm

in the middle so that their relative position in this R&D magnet can be interchanged. All coils had one 8.5 mm thick end spacer after 5 turns (counting from the inner radius) to reduce the peak field in the ends below the peak field in the cross-section. In addition, there was one wedge in the magnet cross section, also 8.5 mm thick and continuous with the end spacer in the return end.

The degradation in I_c of Nb_3Sn as a function of strain in various background fields has been measured by Ekin [9]. Bending degradation is a function of strain and magnetic field, particularly at the high fields (field over 10 T). Therefore for "React & Wind" high field magnet technology, it is important to develop a magnetic design that has low bending strain. In order to minimize bending strain, the bending radii of the coils should be large and the diameter of the Nb_3Sn wires should be small. The guideline for this design was to keep the bending degradation in critical current below 15% so that the computed degradation in quench performance is well below 5%. This requires limiting the bending strain to ~0.3% for a 12 T peak field, ~0.25% for a 14 T field and ~0.2% for a 15 T field. However, it may be noted that the peak field and the peak bending strain are not necessarily at the same location (the peak bending strain is at the coil inner radius and the peak field is at the coil midplane of either aperture).

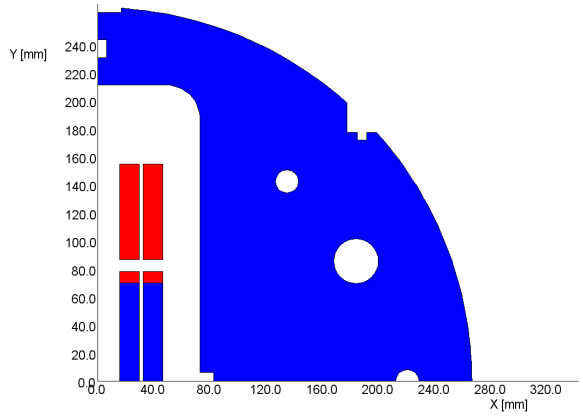

Fig 1. A 2-d model of ¼ of the common coil dipole DCC017.

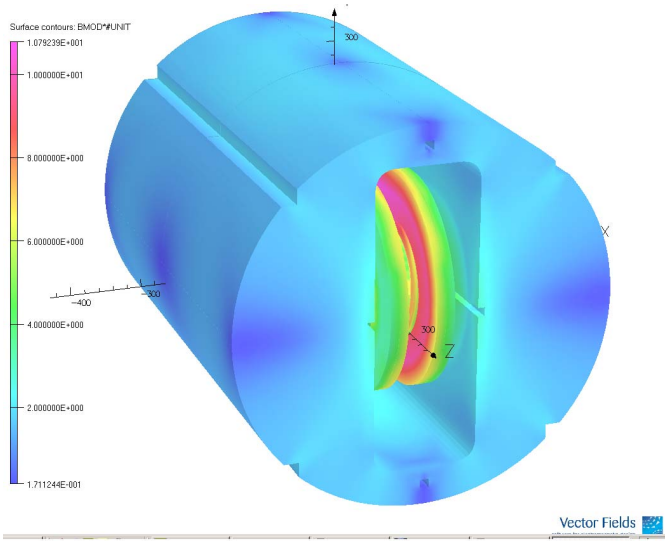

Fig. 2. A 3-d model of the common coil dipole DCC017 with the magnitude of field superimposed on the surface of conductor and iron yoke. The maximum field is in the straight section of the superconducting coil.

The initial design was based on wires in inner and outer layers having different copper to superconductor ratio (0.8 and 1.53 respectively) for grading. The mechanical properties of the inner and outer cables were nearly the same and the necessary grading can be provided by an electrical shunt between inner and outer layer. A variable shunt power supply would have allowed a change in the relative grading during the operation. The shunt was incorporated in the construction

of the magnet, but was not used during the testing. At the time of winding the coils, the outer cable had been successfully tested, giving the desired performance and stability while the inner cable had not been. Also, inspection of the inner cable revealed a higher degree of brittleness which was deemed an indicator of potential problems. Because of this, the choice was made to use the outer cable for both inner and outer layers of the magnet. However, the use of outer cable in both inner and outer layers and the absence of grading significantly reduced the expected short sample field from the original design value of ~12 T. The expected short sample performance of the magnet was 10.2 T based on the actual configuration, cable measurements and inclusion of the computed bending degradation (see next section). The magnet was limited by the inner layer because of a much larger peak field in the inner as compared to that in the outer (see Table I).

The bobbin (or central island) on which the coil is wound was made of magnetic steel (the original design had a 5 mm non-magnetic liner). The use of magnetic steel (a) reduces the peak field on the conductor and (b) also reduces the loss in pre-stress from cool-down because of its lower thermal expansion as compared to other materials (G-10, coil composite, copper) in the magnet structure.

In the cross-section of the common coil magnet, the largest component of the Lorentz force is horizontal and is in the outward direction. The net vertical component of the Lorentz force on the entire coil (pole-to-pole) is small. The direction of the vertical Lorentz force depends on the material of bobbin. In the case of a non-magnetic bobbin the Lorentz forces are vertically outward or away from the bobbin and in the case of magnetic bobbin they are towards the bobbin, at least at low fields. In the present design, the computed horizontal/vertical components of the forces in the first quadrant (right side of the upper aperture of the magnet) are 43MPa/-1.2MPa at 10.2 T (computed quench field), 59MPa/-0.8MPa at 12 T and 77MPa/-0.3MPa at 13.8 T. The magnitude of the vertical force decreases due to saturation of the iron bobbin.

B. Mechanical Design

The overall mechanical structure of the magnet is shown in Fig. 3. The structure was designed [4] to contain Lorentz forces at the original design field of 12 T in a ~40 mm aperture. In this design the horizontal component of the force was 75 MPa. Therefore there is a sufficient margin in the basic support structure since the outward horizontal force in the present configuration at 10.2 T is only 59 MPa. In fact, the present mechanical structure can contain forces for fields over 13.5 T (13.5 T central field is achieved if the present cable is replaced by one with high performance Nb_3Sn wires with a non-Cu critical current density of 3000 A/mm^2).

The 2-d structure was designed for no pre-stress in horizontal or vertical directions. It consisted of a 13 mm thick stainless steel collar, a rigid yoke having a radius of 267 mm and a 25 mm thick stainless steel shell. The end structure consisted of a 127 mm stainless steel end plate. The end plate was circumferentially welded to the stainless shell and can contain an axial load of 1.1 MN (a value at ~12 T in original design). Eighteen set screws constrained the coil ends against 25 mm thick pressure plates. As in the case of the straight section, no pre-load was applied to magnet ends. End saddles and side bars of the coils were made of stainless steel to keep the structure as rigid as possible. The brass spacer was slit at many places to help it follow the layout of cable in the ends and hence minimize the possibility of pinching the brittle cable. All coils were vacuum impregnated individually with end saddles and side bars installed.

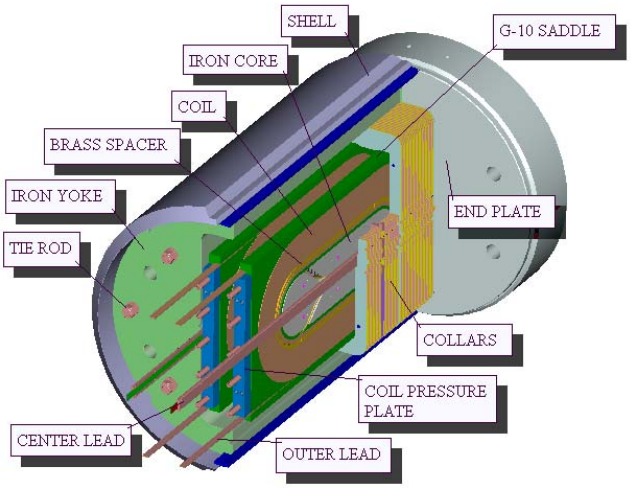

Fig. 3. Overall mechanical layout.

III. Conductor

A. Strand and Cable Parameters

DCC017 used 30-strand cable made from 0.8 mm diameter strand manufactured by Oxford Instruments Superconducting Technology [10] using the Modified Jelly Roll (MJR) process. The Nb_3Sn wire used came from two billets, ORE-163 and ORE-202. Both billets have the same nominal copper fraction of 60%. Coils for this magnet were made from two lengths of cables. Cable BNL-N-4-0012 was fabricated in New England Wire Co. and cable BNL-6-O-B0899R was fabricated at Lawrence Berkeley National Laboratory. All cable lengths for the four coils were vacuum impregnated with Mobil-1®, and pre-annealed at 200^o C for 8 hours to drive-off the volatile constituents in the oil and also to remove the strain in the copper. The use of Mobil1 was found to prevent the sintering of the strands after reaction. This is important, because if the strands were sintered then bending the cable would cause greater strain degradation by about a factor of two. Four ~130 m long sections of cable, were reacted in a vacuum furnace using the following schedule: 48 hrs/200 ^{o} C + 48 hrs/400 ^{o} C + 72 hrs/665^o C. After reaction the width, and mid-thickness of cable BNL-N-4-0012 (used in coil 32) were respectively 12.72 mm, and 1.509 mm and for cable BNL-6-O-B0899R (used in coils 33, 34 and 35) were respectively 13.17 mm, and 1.513 mm.

B. Strand Tests

Extracted strands from the cable were reacted on stainless

barrels using the same reaction schedule as the cable segments. The critical current measurements of the extracted strands (ORE-163 with Cu/non-cu ratio of 1.54 and ORE-202 with Cu/non-cu ratio of 1.6) were carried out in the range of 8 T to 11.5 T. These measurements are used in computing the critical current of the cable at 4.2 K, which is summarized in Table II. To fit measured data, we used Summer's formulation [11] with the following parameters: ε=-0.016, B_{c2m}=27.6 T and T_{co}=17.8 K. This allows one to extrapolate beyond the range of fields measured and it can be used to calculate the critical currents for a different temperature or a different relative strain. Strand data are multiplied by 30 to calculate the cable I_c, as given in Table II.

TABLE II
EXPECTED PERFORMANCE OF CABLE USED IN COMMON COIL DIPOLE DCC017. "*FITTED*" REFERS TO THE STRAND MEASUREMENTS AT 4.2 K MULTIPLIED BY NUMBER OF STRANDS (30) AND "*WITH STRAIN*" REFERS TO THE EXPECTED PERFORMANCE AT 4.5 K IN MAGNET WITH ADDITIONAL STRAIN OF -0.21% DUE TO BENDING, COMPUTED USING SUMMER'S FORMULATION.

	Cable BNL-N-4-0012 (used in coil 32)		Cable BNL-6-O-B0899R (used in coil 33, 34 and 35)	
H, T	I_c (fitted)	I_c (with strain)	I_c (fitted)	I_c (with strain)
9.0	19710	16077	21348	17458
9.5	17970	14383	19404	15687
10.0	16260	12838	17618	14068
10.5	14649	11427	15975	12587
11.0	13188	10137	14462	11230
11.5	11820	8959	13065	9986
12	10650	7882	11776	8847

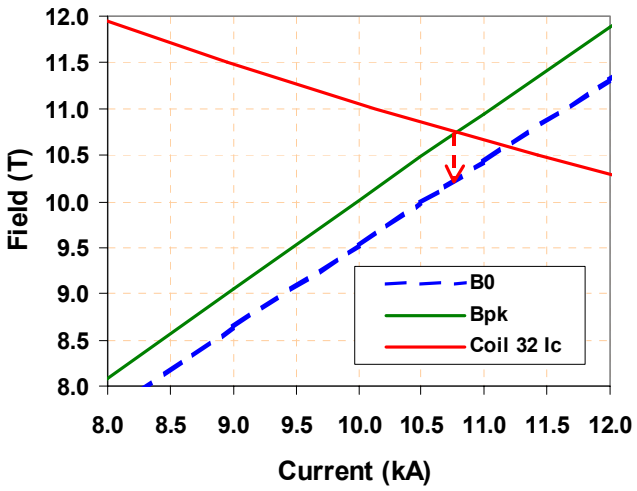

Fig. 4: Critical surface, peak field and load line in magnet DCC017.

The cable was reacted on a 280 mm diameter stainless steel drum. Therefore, after coil winding the bending strain experienced by the strand when (a) the cable from the drum is straightened and (b) when the cable is bent at radius of 70 mm are of nearly the same in magnitude but opposite in sign. The effect of the bending is to add tensile strain along the outside of the strand and the same magnitude of compressive strain along the inside of the strand. The magnitude of the bending strain is equal to r/R, where r is the radius of the filament boundary in the strand (0.58 mm) and R is the bending radius. Since the strand is reacted at a radius of 140 mm, the effective bending radius when the cable is bent at a radius of 70 mm is 140 mm (since the change in 1/R is 1/70 – 1/140 = 1/140). From the as-reacted state, the strand J_c increases with tension and decreases with compression strain [9]. Bending increases the compressive strain in the strand from the "as-reacted" state by 0.21%. The minimum I_c of the strand/cable is then calculated using Summer's fit [11] and changing the strain by -0.21%. In the absence of direct measurements the calculated I_c sets a lower bound for the effect of bending strain. Since coil 32 is one of the inner coils, it will be the limiting coil when the magnet reaches the short sample limit. The calculated critical currents at 4.2 K and the strain-degraded current at 4.5 K are shown in Table II .

Fig. 4 shows the load line and the critical current of the cable in coil 32 at a temperature of 4.5 K and a strain $\Delta\varepsilon$=-0.21%. This gives a short sample limit of 10.8 kA using the computed peak field load line based on 2-d and 3-d models. This corresponds to a peak field of 10.7 T on conductor and a central field of 10.2 T in both apertures.

IV. TOOLING

Since the pre-reacted Nb_3Sn conductor is brittle and sensitive to local strain, manual handling must be minimized to avoid accidental damage or degradation. Therefore, to minimize handling and bending degradation good design and reliable operation of the coil winding tooling is important in developing "React & Wind" technology. The BNL coil winding tooling is shown in Fig. 5. Other major pieces of tooling developed for this program were the coil impregnation fixture and the coil collaring press.

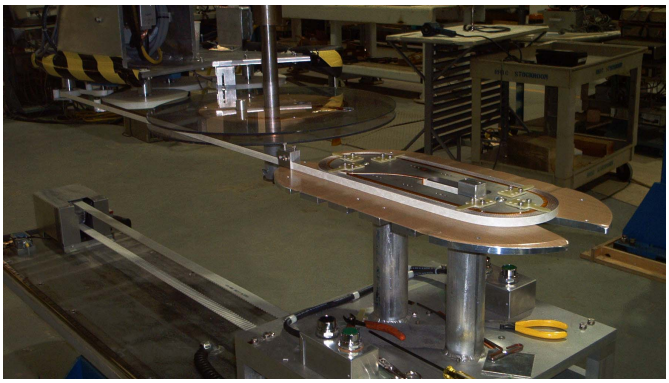

Fig. 5: Coil winding tooling.

V. CONSTRUCTION

Four coils were wound with pre-reacted 30-strand Nb_3Sn cable on a magnetic steel flat racetrack bobbin having a straight section length of 300 mm and a bending diameter of 70 mm. The turn-to-turn insulating separator was Nomex® ~170 micrometer thick and ~13.2 mm wide (approximately the same width as the cable). Utmost care was taken to avoid over-straining the cable. The winding tension did not exceed 53 N (12 lb) for the cable and 67 N (15 lb) for the Nomex®. No clamps were used during winding. The cable was permitted to make its natural transition from straight section to

end. The cable assumed an angle of 7° with respect to vertical as measured at the 45th turn because of a small difference in the thickness of cable from edge to edge. No attempt was made to remove this condition due to overriding concerns regarding possible conductor damage. A minimal 222 N (50 lb) force was applied to the straight section of the coil to set its width and requisite shimming against the bobbin. All shims were tapered at the ends of the straight section to follow the shape of the cable turn.

The end saddles and side bars were made of stainless steel and were custom fit to each individual coil. No pre-compression was applied during coil impregnating or curing. All large voids were filled with fiberglass or G-10. Each coil was checked for straightness and flatness after curing. The coils were pinned into pairs and shimmed to equal overall size with alumina filled epoxy. Stainless steel sheets having a thickness of 1.65 mm were placed between the layers of each coil pair to aid in stress distribution at full power. Four 25 micrometer thick stainless steel strip heaters insulated with Kapton® were placed on both sides of this sheet. They were installed between each paired coil assembly to aid quench protection. One of the two coil modules consisting of a pair of coils is shown in Fig. 6. This assembly contains an internal splice made with a set of (twelve) perpendicular Nb-Ti cables. Nb-Ti could be used since, in the common coil design, the field is low in this splice region. A shunt lead (coming out axially in the middle) can also be seen in Fig. 6. Shunt lead contained Nb_3Sn cable since it passes through a relatively higher field region in the ends.

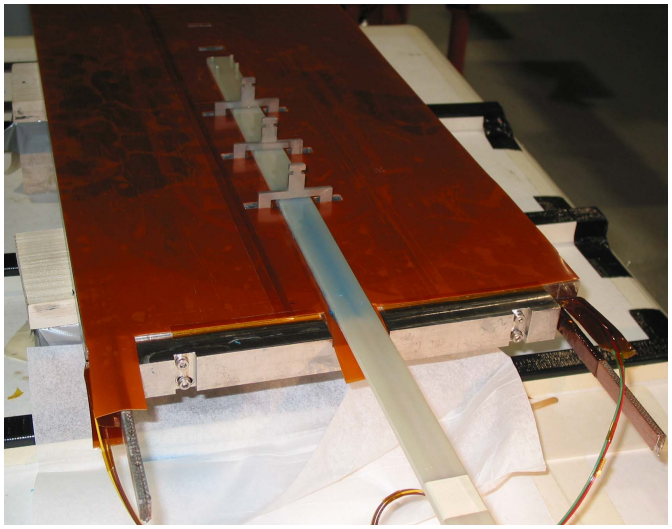

Fig. 6. Coil modules consisting of a pair of coils and the shunt lead.

A collaring press was built specifically for this magnet. It is sufficiently massive and stiff to limit coil bending and/or twisting to safe levels. Coil pre-stress was strictly in the side-to-side direction (cable stack direction) and was relatively low (17 MPa or 2.5 kpsi). An inflatable bladder was employed to maintain the coils hard outward against the collars during collaring. Stainless steel "keepers" were installed for the purpose of locking the coils against the collars.

The laminated iron yoke, along with the 25.4 mm thick stainless steel shell, serves to support the collars at mid-span in resisting the lateral Lorentz forces generated by the coils. The goal was to keep the axial strain due to the end Lorentz forces less than 0.2% by the use of 127 mm thick end plates.

VI. Magnet Test

A. Experimental Setup and Test Procedure

The magnet test [12] was performed at the Vertical Test Facility in a liquid helium bath at a nominal temperature of 4.5 K. The magnet was instrumented with voltage taps located between the coils and at the leads to the coils so that the voltages of the four coils could be monitored during testing. Quenches were detected by monitoring the voltage difference between the coil pairs and generating a stop pulse when the voltage exceeded a set threshold voltage level. An additional quench detection circuit used the difference between the total coil voltage and the current derivative voltage signal. There were no voltage taps in the body of the coils.

It was determined by quench propagation calculations, using the program QUENCH [13], that quench hot spot temperatures could exceed 400 K, where degradation of the Nb_3Sn cable could begin to occur due to thermo-mechanical strain effects [14]. Calculations also give the relationship between the quench temperature, which is not directly measurable, and the quench integral quantity $\int I^2.dt$, which is easily measured. It was decided to limit the quench temperature to 300 K where the quench integral limit in MIITS is 21. Since energy extraction was not available for this particular test, it was therefore necessary to provide an active quench protection scheme to avoid a strain problem during quench tests. For quench protection, the coils were instrumented with quench protection heaters. These consisted of two type 304 stainless steel strips each of thickness 0.0254 mm and width 38.1 mm separated by 6.35 mm. They were installed between the layers in each coil pair and positioned along each side of the inside surfaces of each layer. The strips were mounted on both sides of the Kapton®-wrapped stainless steel sheet which separated the layers of each coil pair and essentially prevented quench propagation between the layers. Additionally the strips were separated into two circuits each with its own power supply for redundancy.

Each strip heater circuit fired on a stop pulse from the quench detector. A capacitance of 21700 μF provided the heater circuit 450 V and 105 A peak to quench the coils. The insulation (Kapton with adhesive, fiberglass, and CTD-101K epoxy) was as much as 1.07 mm thick between the heater strips and the bare conductor. There was no copper shunting provided on the stainless steel. Quench delay times at 4000 A after heater-firing were measured as 100 – 200 ms due to the thermal diffusion barrier across the insulation.

Quench tests were performed by powering the magnet in the common coil electrical configuration using a 30 kA 15 V power supply. Current ramps were done at rates from 3 A/s to 200 A/s with most quenches done at 25 A/s or less. On detection of a quench, a stop pulse from the quench detector

shut off the power supply, fired the strip heaters, and triggered the fast data logger system to acquire voltage signal data at 1 kHz sampling rate.

B. Test Results

Fig. 7 shows the complete quench history, which included a thermal cycle and a ramp rate study at the end. A total of 66 quenches were done, with 38 before the thermal cycle. There were 16 quenches during initial training to just under 10 kA. As can be seen from the plot, quench behavior was then erratic with quench currents varying from 8699 A to 10475 A. After the thermal cycle, the behavior was significantly less erratic with most quench currents above 10 kA and reaching 10846 A (10.2 T central field), which is slightly above the calculated short sample limit, as can be seen from Fig. 4, which shows the cable characteristics and the magnet load line. The highest current quenches were in coil 32, whose conductor had a slightly lower critical current density and which was predicted to reach its conductor limit before the other coils. The highest quench currents were also at the 200 A/s ramp rate, but from the plot it is unclear that there is a ramp rate dependence.

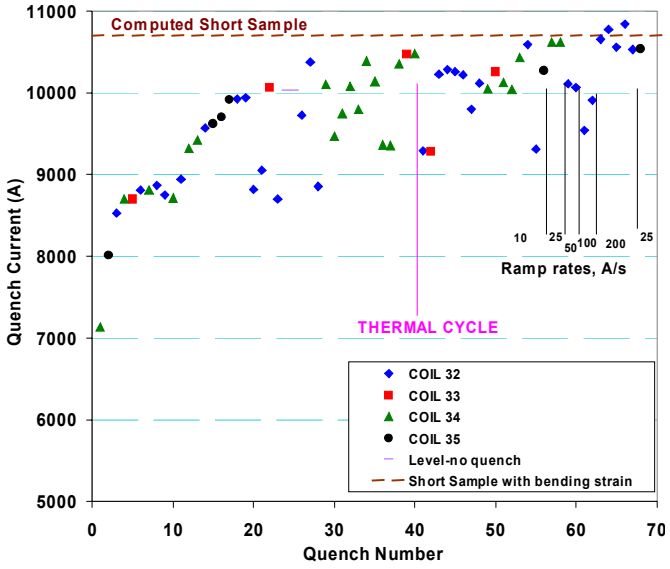

Fig. 7: Complete quench history of "React & Wind" common coil dipole magnet DCC017. Short sample limit line is drawn at 10,800 A which corresponds to a peak field of 10.7 T and central (bore) field of 10.2 T.

The locations of the training and erratic quenches took place in all four coils. Measurements of the initial slope of the voltage increase gave values of dV/dt which varied from 6 V/s to 100 V/s and showed no correlation with quench current, with different values of dV/dt resulting from similar quench currents. This implies that locations within the coils varied. Pre-quench voltage spike detection was limited to a resolution of 60 mV and 1 ms. Most quench signals exhibited voltage spikes, some of which were recognized as due to flux jump instability, but very few quenches exhibited spikes right at quench onset, at least above 60 mV.

Starting with quench #46, the delay between the quench detector stop pulse and power supply shutoff/strip heater trigger was 16 ms. Prior to this quench, the delay was about 58 ms. This was done by inhibiting the power supply firing circuit. The delay was minimized in order to decrease the amount of heating in the coils after each quench. Before this values of the quench integral were more often above 16 MIITS, with a maximum reached of 19.1. According to the quench propagation calculations, this corresponded to a quench temperature of about 220 K, which was well below the safe limit of 300 K.

VII. Conclusion And Summary

The construction and test results of this magnet demonstrate the viability of "React & Wind" magnet technology in high field Nb_3Sn magnets. "React & Wind" magnet technology is particularly attractive in building long production magnets in industry. With a proper magnet design and tooling, one should be able to build Nb_3Sn "React & Wind" magnets up to a field of 15 T. Future potential uses of this magnet include incorporating "React & Wind" HTS coils with BSCCO 2212 Rutherford cable in a high field hybrid structure.

Acknowledgment

We acknowledge the contributions of our technical support staff in design, construction and testing of this magnet.

References

[1] R.C. Gupta, "A Common Coil Design for High Field 2-in-1 Accelerator Magnets," *Particle Accelerator Conference*, pp 3345-3347 (1997).

[2] R. Gupta, et al., "Common Coil Magnet Program at BNL," *IEEE Trans. on Appl. Supercond.*, Vol. 11, Issue 1, Part 2, pp 2168–2171 (2001).

[3] J. Escallier, et al., "Technology Development for React and Wind Common Coil Magnets", *Particle Accelerator Conference*, pp 214-216 (2001).

[4] J. Cozzolino, et al., "Magnet Engineering and Test Results of the High Field Magnet R&D Program at BNL," *IEEE Trans. on Appl. Supercond.*, Vol. 13, Issue 2, Part 2, pp 1347-1350 (2003).

[5] G. Ambrosio, et al., "Design, modification, fabrication, and test of HFDB-03 Racetrack Magnet wound with Pre-Reacted Nb_3Sn Rutherford Cable," *Advances in Cryo. Engineering*, Vol. 49 (2003).

[6] V.S. Kashikhin, et al., "Development and Test of Single-Layer Common Coil Dipole Wound with Reacted Nb_3Sn Cable," *IEEE Trans. on Appl. Supercond.*, Vol. 14, Issue 2, pp 353–356 (2004).

[7] W.B. Sampson, et al., "Nb_3Sn Dipole Magnets," *Trans. of Magnetics*, Vol. MAG-15, p. 117 (1979).

[8] W.B. Sampson, "Nb_3Sn High Field Dipole," *Trans. of Magnetics*, Vol. 27, No. 2, pp 1193-1195 (1991).

[9] J. W. Ekin, "Strain Scaling Law for Flux Pinning in Practical Superconductors. Part 1: Basic Relationship and Application to Nb_3Sn Conductors," *Cryogenics*, 20, p. 611 (1980).

[10] J. A. Parrell, Y. Zhang, R. W. Hentges, M. B. Field and S. Hong, "Nb_3Sn strand development at Oxford Superconducting Technology", *IEEE Trans. Appl. Supercond.*, vol. 13, pp. 3470-3473, June 2003.

[11] L.T. Summers, M.W. Guinan, J.R. Miller, and P.A. Hahn, "A Model for the Prediction of Nb_3Sn Critical Current as a Function of Field, Temperature, Strain and Radiation Damage," *IEEE Transaction on Magnetics*, Vol. 27, No. 2, p. 2041 (1991).

[12] M. Anerella, J. Cozzolino, J. Escallier, G. Ganetis, A. Ghosh, R. Gupta, M. Harrison, P. Joshi, W. Louie, J. Muratore, P. Wanderer, "Construction and Test of Nb_3Sn Common Coil Magnet DCC017," *Magnet Division Internal Note* No. MDN-644-33 (unpublished), 2006.

[13] M. Wilson, "Superconducting Magnets," *Oxford Univ. Press*, (1983).

[14] L. Imbasciatti, "Studies of Quench Protection in Nb_3Sn Superconducting Magnets for Future Partical Accelerators," PhD Thesis *and Fermilab Technical Division Note* TD-03-028 (unpublished), (2003).